



Real-time optical thickness determination for producing ultra-thin silicon membranes using anisotropic potassium hydroxide etching

Leif Gislason¹ · Sahra Genc¹ · Sally Thompson¹ · Jerry Crawford¹ · Jeff Jessing¹

Received: 5 June 2024 / Accepted: 15 September 2024
© The Author(s) 2024

Abstract

Thinning silicon wafers via wet etching is a common practice in the microelectromechanical system (MEMS) industry to produce membranes and other structures Wang (Nano Lett 13(9): 4393–4398, 2013). Controlling the thickness of a membrane is a critical aspect to optimize the functionality of these devices. Our research specifically focuses on the production of bio-membranes for lung-on-a-chip (LoaC) applications. In our fabrication, it is crucial for us to determine the membranes' thickness in a non-invasive way. This study aims to address this issue by attempting to develop a tool that uses the optical properties of light transmission through silicon to find a correlation with thickness. To find this correlation, we conducted a small experimental study where we fabricated ultra-thin membranes and captured images of the light transmission through these samples. This paper will report the correlation found between calculated average intensities of these images and measurements done using scanning electron microscopy (SEM).

Introduction

Anisotropic aqueous etching with potassium hydroxide is a commonly used technique for micromachining silicon in MEMS applications [2, 3]. Real-time estimation of thickness during the fabrication process of thinning silicon is critical for achieving the desired structure [4–7]. However, most of the reported in situ measurement techniques are destructive and complex, thus not amiable to deployment [8, 9]. There is a need for estimating the thickness nondestructively for optimal utilization of this thinning process in a large variety of applications.

Our group is focused on fabricating ultra-thin, porous silicon bio-membranes for LoaC systems with the goal to develop a better understanding of disease pathology and personalized medicine [10]. In our membrane fabrication process, we utilize potassium hydroxide (KOH) for thinning purposes and employ electrochemical anodization to create pore structure in the silicon [11]. The target membrane thickness required for LoaC applications is approximately 1.1 μm , i.e., the interstitial membrane thickness found within the human lung [10, 11]. For the duration of our research, we

had the obstacle of estimating the thickness of thinned membrane noninvasively which is essential before proceeding with electrochemical anodization process. To address this problem, we developed a method that uses light transmission properties of silicon to determine sample thicknesses precisely. This technique calculates the intensity of light from a highly uniform source that is transmitted through a thinned sample and then outputs the membrane thickness. An exponential regression model forms the basis of the predictive model. Overall, this method eliminates the need for destructive measurement techniques, such as cross-sectioning. This work outlines the development of this tool and reports the correlation found between the intensity of light transmission and corresponding silicon membrane thickness.

Materials and methods

Membrane preparation

An initial set of membranes with a range of thicknesses were prepared for use as the input for the predictive exponential regression model. *P*-type, (100), double-sided polish, silicon wafers with initial thickness of $230 \pm 25 \mu\text{m}$ and resistivity of 0.01–0.1 $\Omega\text{-cm}$ were used in this study. Standard solvent-cleaned silicon wafers undergo a wet etching process using a solution containing 600 g of KOH dissolved in 600 mL of

✉ Jeff Jessing
jrjessing@fortlewis.edu

¹ Department of Physics and Engineering, Fort Lewis College, Durango, CO, USA

deionized water (50 wt%). The prepared solution is evenly heated in an isothermal bath as shown in Fig. 1. Wafers are placed in a custom-fabricated polytetrafluoroethylene (PTFE) holder that is then submerged into the 90 °C KOH solution where the chemical thinning process begins. After a calculated time, the thinning sample is quenched in three deionized water baths (each at progressively lower temperatures) and carefully dried with a nitrogen gun. This method or slight variations of the method can yield membranes down to under 1 μm . It is on the thin side of this range that the optical end-point technique has significant benefit, as discussed below.

Optical setup and physical thickness determination

The optical setup consists of a Nikon D750 camera, a highly uniform light emitting diode (LED) Advanced Illumination (Rochester, VT) panel light source, and a custom-fabricated enclosure that has an aperture opening on both sides. The camera is equipped with a Nikkor AF-S 120-mm lens with +6 close-up filters to allow a small working distance (*i.e.*, close focus). The sample is aligned parallel to the camera, with an 11.5-cm gap between them. Images are captured in a dark room to minimize extraneous light. Camera settings are selected to minimize noise, maximize resolution, and most importantly to provide a standardized exposure (*e.g.*, aperture of f11, iso 100, a shutter speed of 1/2.5s). This standardized exposure was selected experimentally to allow thickness determination from approximately 0.5 μm to 20 μm . The optical setup is shown in Fig. 2a.

After the samples are thinned to a target thickness, they are marked with DAG-T-502 carbon paint from Ted Pella, Inc. (Redding, CA) (see Fig. 2b) to allow for localization of the optically collected data with the subsequent cross-sectional thickness measurements determined using electron microscopy. The carbon paint is applied to the membrane surface using single strands of a small paint brush yielding fine lines. After the application of the carbon paint markings that are roughly 1 mm thick with 3-mm gaps between each, the sample is baked at 150 °C in a convection oven. The carbon markings on the membranes allow for correlation of optical thickness to physical (SEM) thickness by providing four regions between the lines. Specifically, following the optical transmission imaging (Fig. 2b), the samples are cleaved perpendicular to the carbon paint marks where one-half of the sectioned sample is placed into a JEOL 7100F SEM for cross-section thickness measurements where each of the four inter-line sections have 20 thickness measurements spanning the entire region (*i.e.*, from carbon line to line). The error of thickness is calculated by the standard deviation of these 20 measurements. A representative SEM cross-section measurement is shown in Fig. 2c.

Intensity determination and thickness estimation

The images taken in the optical setup are imported into a Python code where they are first converted to grayscale and an intensity value is calculated for each pixel. An example image that is converted to grayscale is shown in Fig. 3. The average intensity is calculated by summing all the intensity

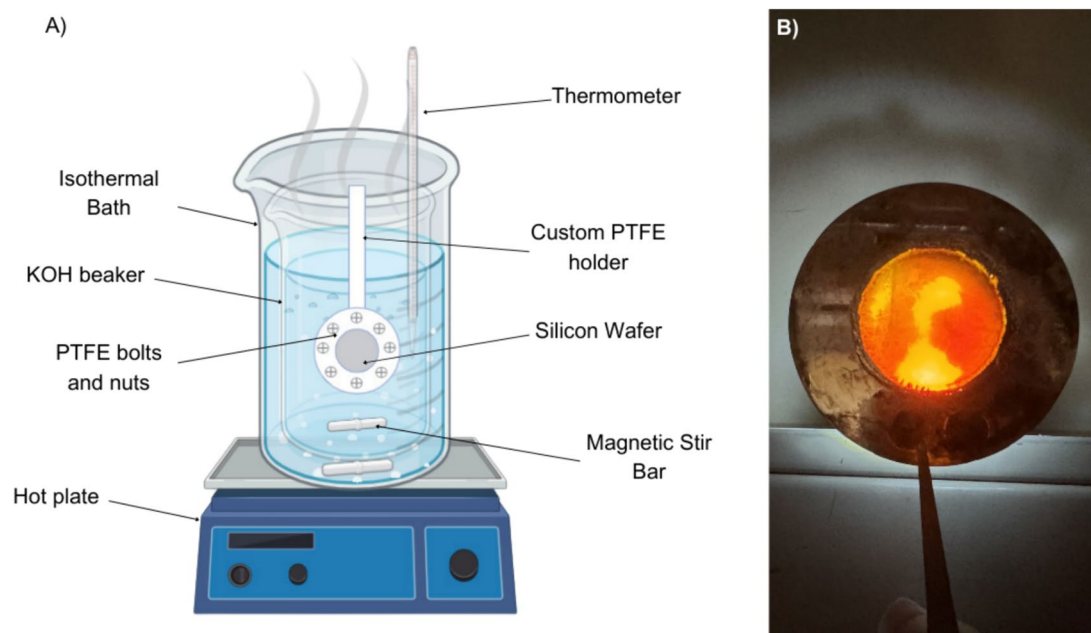
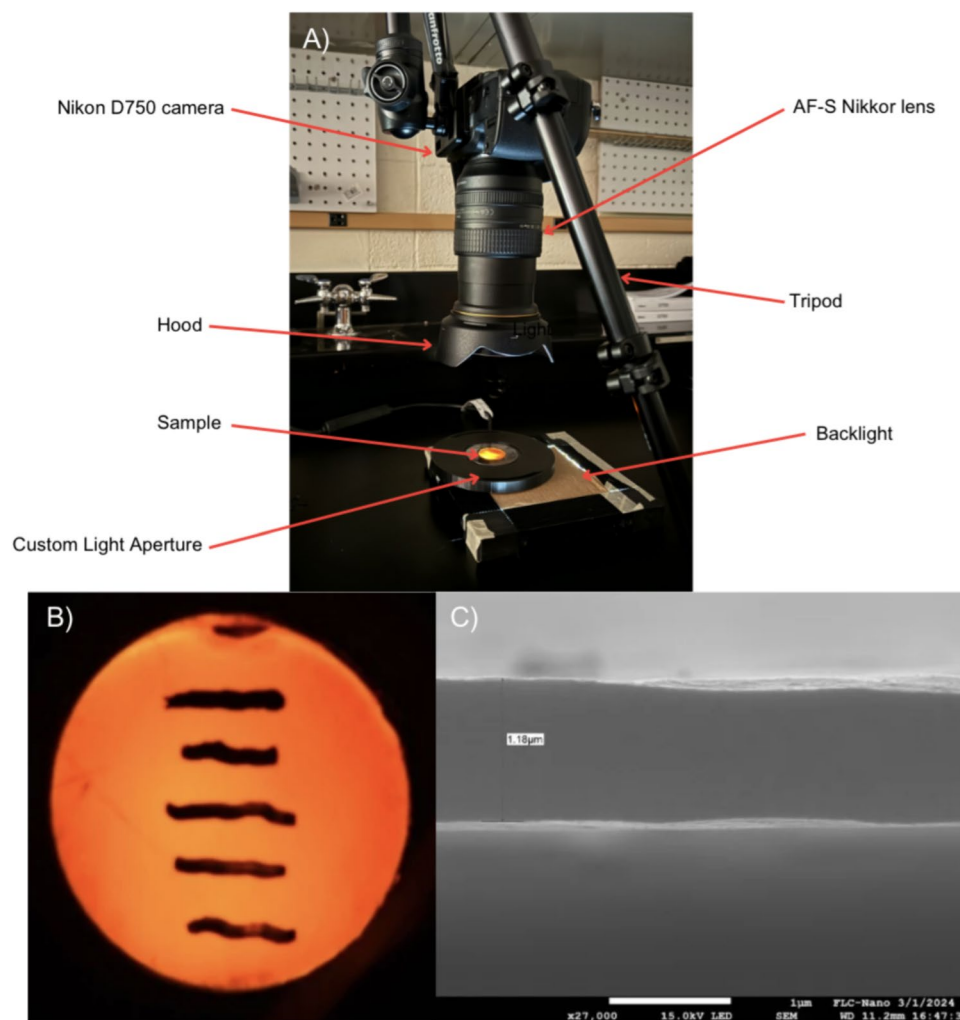


Fig. 1 a KOH anisotropic aqueous etch setup. b An example of a thinned membrane (approximately 5 μm thick)

Fig. 2 **a** Optical setup consisting of a light source, sample, camera/lens, and the custom-fabricated sample enclosure/aperture, **b** silicon membrane with carbon paint showing transmitted light, and **c** a single-point SEM thickness measurement (~1.2- μm membrane)



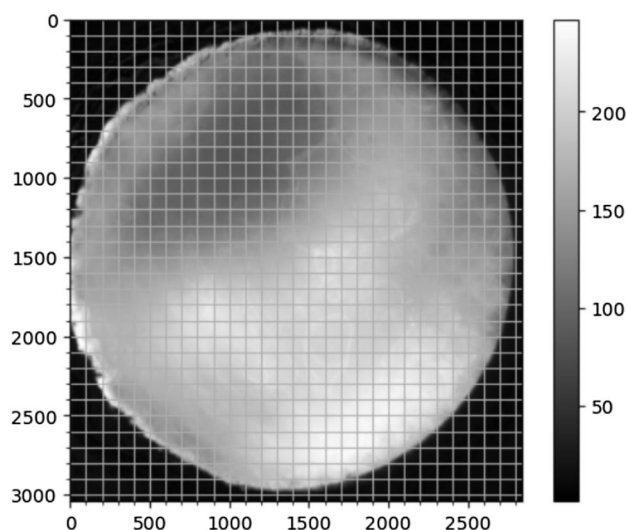
values and dividing them by the number of pixels in the image field. Since care was taken to fix the exposure conditions, there exists a relationship between intensity (*i.e.*, optical thickness) and physical thickness from the SEM cross-sections.

Exponential regression is used to model the relationship between thickness and intensity. The model is developed from the calculated average intensity and the corresponding thickness measurements from samples, as previously described. The error for the average intensity is calculated by taking the standard deviation of the grid points (each 50×50 pixels) as shown in Fig. 3. The model is used to calculate the slope and intercept of the best-fit line (from a semi-log plot) and the calculated values can be used to estimate the thickness of a sample based on its intensity.

Results and discussion

Figure 4 shows the natural logarithm of membrane-transmitted optical intensity [I] versus physical thickness [T] as generated by the Python code, as described above. An exponential regression is shown graphically in the plot and Eq. (1) represents the fit line with an R^2 value of 0.947. As expected from Beer's Law, the fit exhibits an exponentially decaying relationship between the light intensity and the sample thickness.

$$\ln(I) = -(0.222 \pm 0.007)T + \ln(5.819 \pm 0.038) \quad (1)$$



The average intensity for the image is 134.4786
The estimated thickness is 5.7884 μm

Fig. 3 Example optical images after it is converted to grayscale. The x- and y-axes are in relative coordinates. The grayscale values span from 0 (black) to 255 (white), as shown on the right-hand side

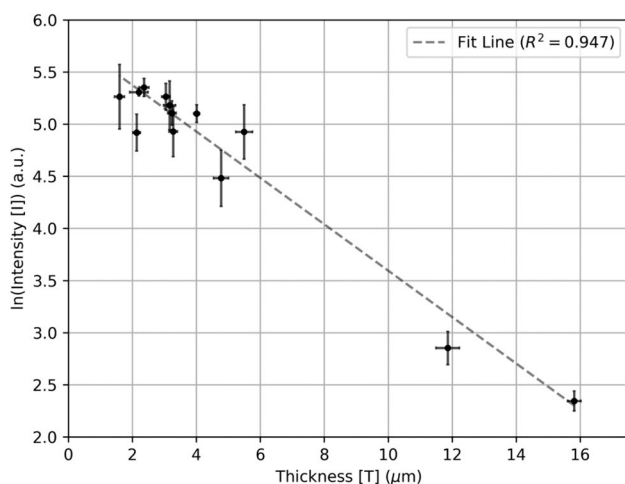


Fig. 4 Sample thickness [T] in microns with respect to the natural logarithm of grayscale light intensity [I]. Y-axis error bars are determined from the standard deviation of 50×50 (pixel) grid intensity. X-axis error bars are determined from the standard deviation of 20 thickness measurements from the SEM

Equation 1 describes how light transmission [I] changes in response to a change in thickness [T] where the rate of change is -0.222 and the y-intercept is 5.819. The thickness represented by the data points ranges from approximately 1 μm to 15 μm with a total of 13 data points. As seen in the presented data, there is an exponential decay in light intensity with silicon thickness.

Future work will be focused on adding more data points, hence providing more inputs for a predictive model

and localization of the correlation between the optical and physical thicknesses will be addressed. Additionally, the optical thickness range will be optimized and extended from approximately 25 μm to under 1 μm . The goal of this work is to refine this technique such that we have a relatively high resolution, non-destructive method to measure in situ silicon membrane thickness during wet anisotropic etching. Modifying this method such that it can be integrated into a real-time etch (in etchant solution) end-point detection system will improve the success rate of producing ultra-thin silicon membranes. The non-destructive aspect is critical in producing large bulk silicon membranes that can subsequently be placed in an electrochemical anodization cell for porous silicon formation as the final step in fabrication of a free-standing porous bio-membrane. This study presents a significant step toward developing a simple, deployable measurement tool using light transmission rather than destructive and complex techniques.

Acknowledgments This project was graciously funded by the NSF PREM for Functional Nanomaterials [Award #1827847] and STROBE NSF Science and Technology Center for Real-Time Functional Imaging [Award #1548924].

Author contributions Leif Gislason contributed to Formal Analysis, Data Curation, Investigation, Methodology, Validation, Software, Visualization, Resources, and Writing—Original Draft. Sahra Genc contributed to Formal Analysis, Data Curation, Investigation, Methodology, Validation, Software, Visualization, Resources, and Writing—Original Draft. Sally Thompson contributed to Formal Analysis, Data Curation, Investigation, Methodology, Validation, Visualization, Resources, and Writing—Original Draft. Jerry Crawford contributed to Formal Analysis, Data Curation, Investigation, Methodology, Validation, Visualization, Resources, and Writing—Review and Editing, and Supervision. Jeff Jessing contributed to Formal Analysis, Data Curation, Investigation, Methodology, Validation, Software, Visualization, Resources, Writing—Original Draft, Supervision, Project Administration, and Funding Acquisition.

Funding This project was graciously funded by the NSF PREM for Functional Nanomaterials [Award #1827847] supporting Sahra Genc, Sally Thompson, Leif Gislason, and Jeff Jessing; STROBE NSF Science and Technology Center for Real-Time Functional Imaging [Award #1548924] supporting Sahra Genc, Sally Thompson, Leif Gislason, and Jeff Jessing.

Data and custom code availability All data obtained and analyzed during this study are available from the corresponding author upon request. The code used in this study is available [here](#).

Declarations

Conflict of interest All authors declare that they have no known competing financial interests or personal relationships that could have appeared to influence the work reported in this paper.

Open Access This article is licensed under a Creative Commons Attribution 4.0 International License, which permits use, sharing,

adaptation, distribution and reproduction in any medium or format, as long as you give appropriate credit to the original author(s) and the source, provide a link to the Creative Commons licence, and indicate if changes were made. The images or other third party material in this article are included in the article's Creative Commons licence, unless indicated otherwise in a credit line to the material. If material is not included in the article's Creative Commons licence and your intended use is not permitted by statutory regulation or exceeds the permitted use, you will need to obtain permission directly from the copyright holder. To view a copy of this licence, visit <http://creativecommons.org/licenses/by/4.0/>.

References

1. S. Wang et al., Large-area free-standing ultrathin single-crystal silicon as processable materials. *Nano Lett.* **13**(9), 4393–4398 (2013). <https://doi.org/10.1021/nl402230v>
2. G.T.A. Kovacs, N.I. Maluf, K.E. Petersen, Bulk micromachining of silicon. *Proc. IEEE* **86**(8), 1536–1551 (1998). <https://doi.org/10.1109/5.704259>
3. P. Pal, V. Swarnalatha, A.V.N. Rao, A.K. Pandey, H. Tanaka, K. Sato, High speed silicon wet anisotropic etching for applications in bulk micromachining: a review. *Micro Nano Syst. Lett.* (2021). <https://doi.org/10.1186/s40486-021-00129-0>
4. U.M. Mescheder, Ch. Koetter, Optical monitoring and control of Si wet etching. *Sens. Actuators, A* **76**(1–3), 425–430 (1999). [https://doi.org/10.1016/s0924-4247\(99\)00212-5](https://doi.org/10.1016/s0924-4247(99)00212-5)
5. H. Tosaka, K. Minami, M. Esashi, Optical in situ monitoring of silicon diaphragm thickness during wet etching. *J. Micromech. Microeng.* **5**(1), 41–46 (1995). <https://doi.org/10.1088/0960-1317/5/1/008>
6. E. Steinsland, T. Finstad, A. Ferber, A. Hanneborg, In situ measurement of etch rate of single crystal silicon. In *in situ Measurement Rate Single Crystal Silicon* (1997). <https://doi.org/10.1109/sensor.1997.613750>
7. C.-Y. Lee et al., “Real-time monitoring of thickness of silicon membrane during wet etching using a novel surface acoustic wave sensor,” *Proceedings of SPIE, the International Society for Optical Engineering/Proceedings of SPIE*, 2004, <https://doi.org/10.1117/12.544959>.
8. M. Mulato, I. Chambouleyron, E.G. Birgin, J.M. Martínez, Determination of thickness and optical constants of amorphous silicon films from transmittance data. *Appl. Phys. Lett.* **77**(14), 2133–2135 (2000). <https://doi.org/10.1063/1.1314299>
9. R. Swanepoel, Determination of the thickness and optical constants of amorphous silicon. *J. Phys. E Sci. Instrum.* **16**(12), 1214–1222 (1983). <https://doi.org/10.1088/0022-3735/16/12/023>
10. M. Williams, C. Wiens, A. Hamilton, S. Mancha, M. Stalder, K. Vargas, J. Crawford, Y. Li, S.M. Schreiner, D. Blake, J.R. Jessing, “Novel Fabrication Approach of a Porous Silicon Biocompatible Membrane Evaluated within a Alveolar Coculture Model,” 2021, <https://doi.org/10.31224/osf.io/mztyc>.
11. S. Genc, S. Thompson, O. Hill, L. Gislason, D. Rodriguez, F. Showme, A. Motler, S.M. Schreiner, A.A. Gestos, V.L. Ferguson, J. Jessing, Morphological and mechanical characterization of a novel porous silicon membrane used in a lung-on-a-chip system. *MRS Adv.* (2023). <https://doi.org/10.1557/s43580-023-00667-2>

Publisher's Note Springer Nature remains neutral with regard to jurisdictional claims in published maps and institutional affiliations.